We are IntechOpen, the world's leading publisher of Open Access books Built by scientists, for scientists

4,800
Open access books available

122,000
International authors and editors

135M
Downloads

Our authors are among the

154
Countries delivered to

TOP 1%
most cited scientists

12.2%
Contributors from top 500 universities

CLARIVATE ANALYTICS BOOK CITATION INDEX INDEXED

WEB OF SCIENCE™

Selection of our books indexed in the Book Citation Index in Web of Science™ Core Collection (BKCI)

Interested in publishing with us?
Contact book.department@intechopen.com

Numbers displayed above are based on latest data collected.
For more information visit www.intechopen.com

Chapter 7

Reciprocating Mechanism–Driven Heat Loop (RMDHL) Cooling Technology for Power Electronic Systems

Olubunmi Popoola, Soheil Soleimanikutanaei and Yiding Cao

Additional information is available at the end of the chapter

http://dx.doi.org/10.5772/62518

Abstract

The most significant hindrances to the technological advances in high power electronics (HPE) and digital computational devices (DCD) has always been the issue of effective thermal management. Energy losses during operation cause heat to build up in these components, resulting in temperature rise. Finding effective thermal solutions will become a major constraint for the reduction of cost and time-to-market, two governing factors between success and failure in commercial evolution of technology. Even when high temperatures are not reached, high thermal stresses because of temperature variations are major causes of failure in electronic components mounted on circuit boards. An effective electronic cooling technique, which is based on reciprocating heat pipe, is the so-called reciprocating mechanism–driven heat loop (RMDHL) that has a heat transfer mechanism different from those of traditional heat pipes. Experimental results show that the heat loop worked very effectively and a heat flux as high as 300 W/cm^2 in the evaporator section could be handled. In addition to eliminating the cavitation problem associated with traditional two-phase heat loops, the RMDHL also provides superior cooling advantage with respect to temperature uniformity. Considering the other advantages of coolant leakage free and the absence of cavitation problems for aerospace-related applications, the single phase RMDHL could be an alternative of a conventional liquid cooling system (LCS) for electronic cooling applications. This chapter will provide insight into experimental, numerical and analytical study undertaken for RMDHL in connection with high heat and high heat flux thermal management applications and electronic cooling. In addition to clarifying the fundamental physics behind the working mechanism of RMDHLs, a working criterion has also been derived, which could provide a guidance for the design of a reciprocating mechanism–driven heat loop.

Keywords: power electronic cooling, high heat flux, reciprocating flow, temperature uniformity, single and two-phase heat transfer

1. Introduction

Thermal management and related design problems continue to be identified by the Semiconductor Industries Association Roadmap [1] as one of the five key challenges during the next decade to achieve the projected performance goals of the industry. Finding effective thermal solutions will become a major constraint for the reduction of cost and time-to-market, two governing factors between success and failure in commercial evolution of technology [2]. In addition to the time urgency, the heat generation problem is further compounded by the increasing trend of miniaturization of these chips. It has been observed over the years, these chips have gotten smaller and more compact and the smaller they get the higher the heat flux associated with their operation. Microelectronic chips may dissipate heat fluxes as high as 10 W through a 5 mm x 5 mm side (400 W/cm^2) [3–5] and heat fluxes over 1,000 W/cm^2 have been projected [6]. As a result, there is a need to create a capability to effectively remove these high heat fluxes. An effective thermal management system must also find a solution to non-uniform system temperature or heat flux distribution across the surfaces [7]. Even when high temperatures are not reached, high thermal stresses because of temperature variations are major causes of failure in electronic components mounted on circuit boards [8]. Non-uniform heat flux distribution leads to local hot spots and elevated temperature gradients across the silicon die, excessive thermal stresses on the device, and ultimately device failure.

For a cooling system, there are several design options to have a larger rate of heat removal. The first option is the passive two-phase heat transfer systems [9, 10]. Some typical passive heat transfer systems are heat pipes, gravity-assisted heat pipes, capillary pumped loops, and vapor chambers (a flat-plate type heat pipe). The passive systems can function without requiring any mechanical power input. However, heat pipe or capillary pumped loop are capable of handling the maximum heat flux of 20 W/cm^2. In some cases for a higher heat flux, a special wick structure design may handle it better but the temperature uniformity requirement may not be held as the temperature drop across the heat pipe could be on the order of 5–10 °C. The capillary pumped loop has an advantage over the heat pipe as it transports heat over a longer distance [11], which is also may considered as a special type of heat pipe. But it may also have the same drawbacks of temperature uniformity and heat flux as heat pipe. The most significant challenge that the above passive heat transfer devices are facing is the tolerance of a substantial body force. In passive heat transfer system, the working fluid could be thrown out of the evaporator because of the inertial force that results in liquid reduction in the evaporator section.

The second option is the single-phase forced convection cooling, which is an active cooling system. This cooling system is the most popular method that uses a pumping system to circulate a liquid coolant for extracting heat from a heat generating device.

The third design option is a two-phase pumped cooling loop to simultaneously satisfy the temperature uniformity and high heat flux requirements [9]. In this case, the coolant is still circulated by a pumping device and the boiling/evaporation are allowed to occur over the heated surface, which could provide an enhanced capability to remove a larger amount of heat and achieve a higher level of temperature uniformity over the system. However, the pumping

http://dx.doi.org/10.5772/62518

reliability is always a serious concern. First, the problem of a large the body force (pΔv stress because of phase change of the coolant) may be experienced during the operation, which may be a significant challenge on the design of a cooling system [12]. Second, the space within the cold plate must be reserved for boiling and vaporization and the two-phase loop cannot be filled completely with the liquid, as a result, vapor or liquid–vapor two-phase mixture may enter the pump, which could cause so-called cavitation problem and render the pump ineffective [13].

There is another heat transfer mechanism different from those of traditional heat pipes called reciprocating heat pipe. Cao et al. [14, 15] developed a reciprocating heat pipe, the so-called reciprocating mechanism–driven heat loop (RMDHL) that worked very effectively. As experimental results show that it can handle a heat flux as high as 300 W/cm^2 in the evaporator section. A RMDHL (**Figure 1**) is normally composed of a hollow loop having an interior flow passage, an amount of working fluid filled within the loop, and a reciprocating driver. The hollow loop has an evaporator section, a condenser section, and a liquid reservoir. The reciprocating driver is integrated with the liquid reservoir and facilitates a reciprocating flow of the working fluid within the loop. It supplies liquid from the condenser to the evaporator under a substantially saturated condition that avoids the cavitation problem associated with a conventional pump. For electronics cooling and high-temperature applications, the reciprocating driver could be a solenoid-operated reciprocating driver (**Figure 1a**) and a bellows-type reciprocating driver (**Figure 1b**), respectively. RMDHL not only eliminates the cavitation problem associated with traditional two-phase heat loops, but also provides superior cooling advantage with respect to temperature uniformity.

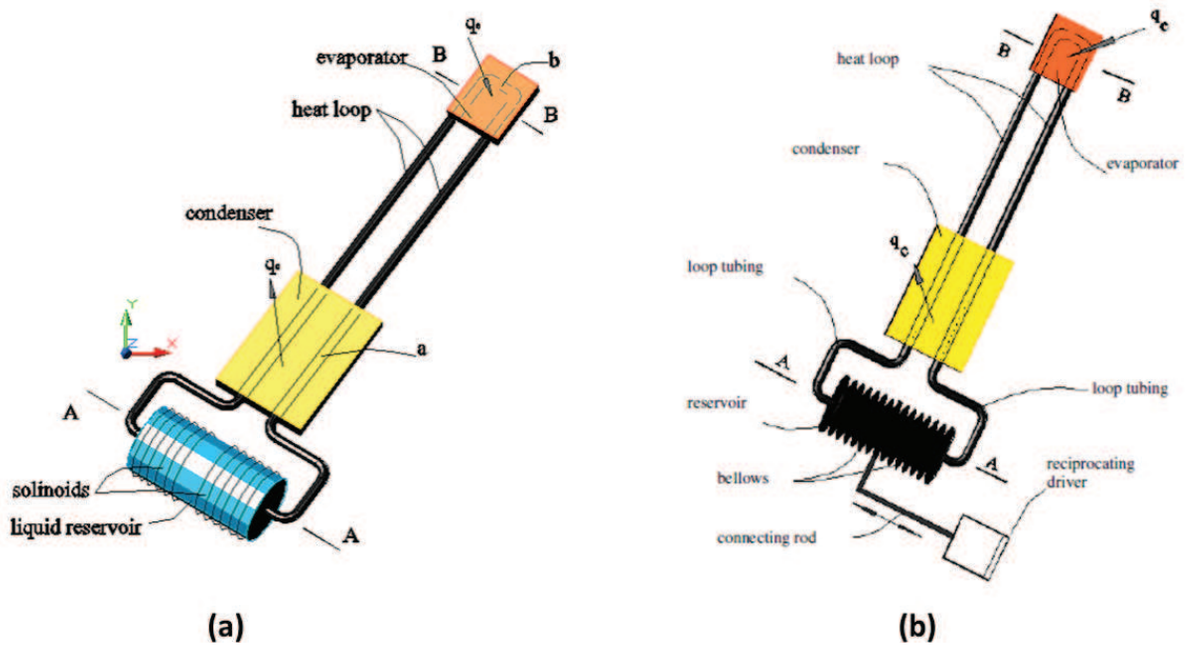

Figure 1. Schematic of a (a) solenoid-driven reciprocating mechanism–driven heat loop and (b) bellows-type reciprocating mechanism–driven heat loop [12].

To facilitate the assembling of the bellows and reciprocating driver, a bellows stand has been constructed and is schematically shown in **Figure 2a**. As seen in the figure, two bellows are placed side by side in a bellows housing. A partition plate between the two bellows holds the two bellows together. The other sides of the two bellows are fixed to the housing plates, respectively, on the frontal and rear sides of the bellows housing. The partition plate is connected to the reciprocating driver through a four-arm rack and four connecting rods that run through the frontal hosing plate. During the operation, the reciprocating motion of the driver arm generates a reciprocating motion of the partition plate, which would then create a reciprocating motion of the working fluid hermetically enclosed within the bellows-type RMDHL. A photo of assembled heat loop under evacuation is shown in **Figure 2b**.

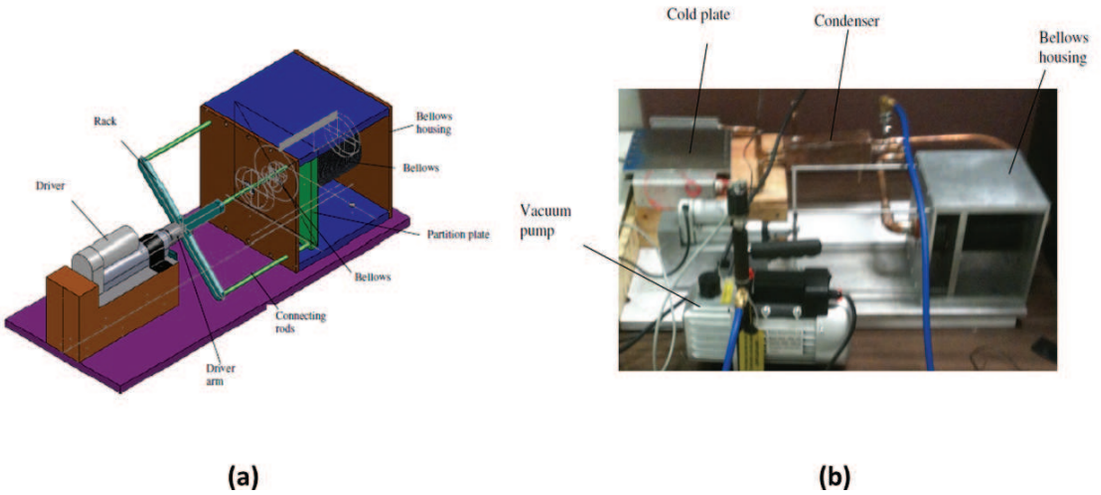

Figure 2. (a) Configuration of the designed bellows/driver assembly. (b) A photo of the assembled bellows-type heat loop being evacuated [9].

Figure 3 illustrates solenoid-operated electromagnetic driver (line A-A in **Figure 1a**), which is composed of a piston of magnetic metal disposed movably inside the reservoir. The circuit of the right-hand solenoid is closed through a switch, whereas the circuit of the left-hand solenoid is opened through a switch associated with it. As a result, the magnetic field generated by the solenoid attracts the piston toward the right that provides a counterclockwise flow of the working fluid within the loop. As the piston approaches the right end of the liquid reservoir, the left-hand switch is closed while the right-hand switch is opened. As a result, the piston is no longer attracted by the right-hand solenoid and instead attracted by left-hand solenoid toward the left which provides a clockwise working fluid flow within the loop. A reciprocating motion of the piston is induced as the circuits of the two solenoids being opened and closed alternately opposite to each other, which produces a reciprocating flow of the working fluid within the heat loop. As the liquid reservoir has a substantially larger inner diameter than that of the loop tubing (or the volume of the reservoir is large compared with the remainder of the interior volume of the loop) and that, a sufficient fraction of the interior volume of the loop is occupied by liquid, with a sufficiently large piston stroke, liquid is effectively supplied to the evaporator section from the condenser section.

http://dx.doi.org/10.5772/62518

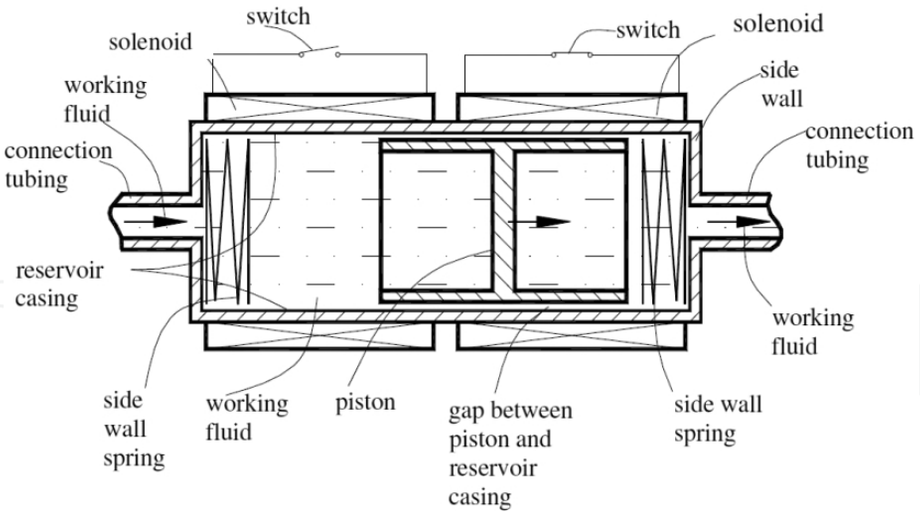

Figure 3. Schematic of a solenoid driver integrated with the liquid reservoir [12].

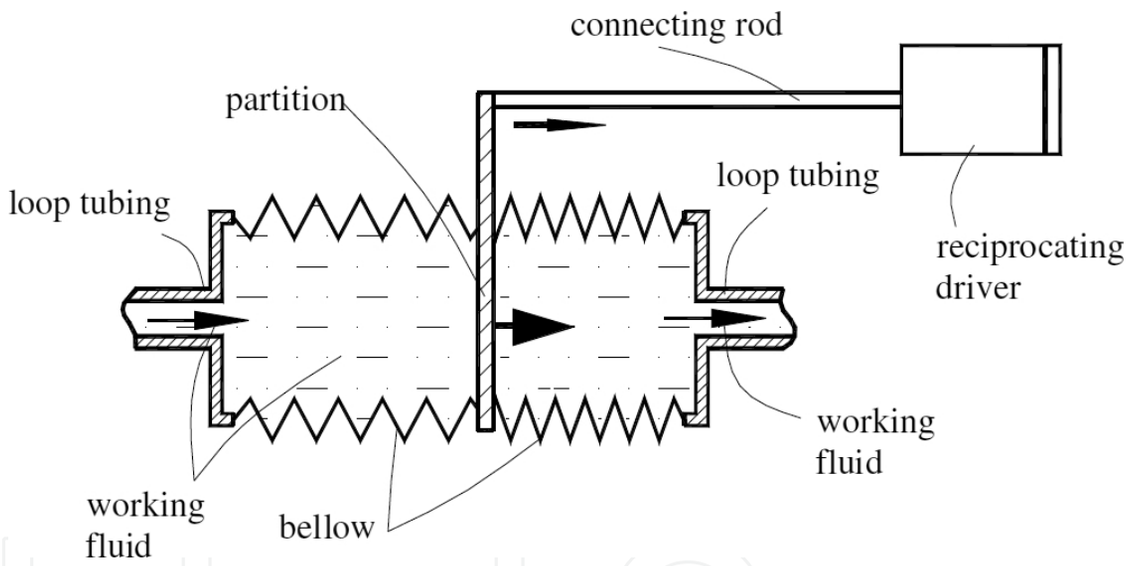

Figure 4. Schematic axial cross-sectional view of a bellows-type reciprocating driver [12].

Figure 4 shows a bellows-type reciprocating heat loop that employs an external reciprocating mechanism as the working temperature of the heat loop is high. As shown in the figure, the bellows is coupled with a reciprocating mechanism through a connecting rod, which could produce a reciprocating motion with a sufficiently large reciprocating stroke. **Figure 1b** shows a detailed description of the aforementioned bellows-type driver in which part or substantially entire circumferential casing of the liquid reservoir is a bellows. A partition is disposed near the mid-section of the bellows. The partition is coupled with an external reciprocating mechanism through a connecting rod. The external reciprocating mechanism can be a solenoid-operated electromagnetic driver or a mechanical reciprocating mechanism driven by an electric motor. As the external reciprocating mechanism is in operation, it generates a recip-

rocating motion of the partition that produces a reciprocating flow of the heat-carrying fluid enclosed within the loop. The bellows-type reciprocating heat loop can work at a much higher temperature as it does not contain any contacting surfaces having a relative motion in the high-temperature region. Additionally, the bellows can be maintained at a sufficiently low temperature for its reliability during the operation as the outer surface of the bellows can be adequately cooled. Moreover, a non-condensable gas can be filled within the bellows to further reduce the bellows temperature.

From the application point of view, a bellows-type RMDHL loop has the advantages over the solenoid-based RMDHL:

1. The bellows-type RMDHL has successfully overcome the weakness of small displacement of a solenoid-based RMDHL, and enabled a RMDHL for applications involving large heat transfer rates and over a large surface area.

2. The tests show that the bellows-type RMDHL has the potential to maintain a heat-generating surface at an exceedingly uniform temperature. Although in some cases, the maximum temperature difference over the cold plate has exceeded 1.5oC, this temperature difference may be significantly reduced with a more powerful actuator working at a higher frequency.

3. The power consumption of the bellows driver was less than 5 W in all cases, resulting in a ratio of the driver power input to the heat input of the cold plate being less than 1%, which is a ten-fold improvement over that of the solenoid-based RMDHL.

In general, a unique advantage offered by the RMDHL is "coolant leakage" free and the absence of cavitation problems for aerospace-related applications. The single-phase RMDHL could also be an alternative of a conventional liquid cooling system (LCS) for electronic cooling applications. We wish to find a relation that could describe this critical requirement for the operation of the heat loop. Parameters to be determined will include the liquid displacement volume of the piston, effective displacement volume of the heat loop, and terminology to describe the mean performance parameters of the RMDHL.

2. Fluid flow specifications

For all cases of the RMDHL, the displacement of the piston $x_p(t)$ with time is [16]:

$$x_p(t) = -\tfrac{1}{2}S - \tfrac{1}{2}S\cos(\omega t) \tag{1}$$

where ω is the pump frequency in radians per second. Differentiating Equation (2) with respect to time we have the mean velocity for the oscillating flow:

http://dx.doi.org/10.5772/62518

$$u = u_{max} \sin(\omega t) \tag{2}$$

The stroke frequency n (in strokes or cycles per second) then follows from:

$$n = \omega / (2\pi) \tag{3}$$

The average volume flow rate q_{av} is equal to the product of stroke volume and pump frequency [16]:

$$q_{av} = \omega / (2\pi) S A_p \tag{4}$$

The pressure gradient takes the form:

$$-\frac{1}{\rho}\frac{\partial p}{\partial x} = a e^{i\omega t} \tag{5}$$

There are several fundamental differences between the reciprocating flow and the continuous flow. First the velocity profiles are completely different. Although the maximum axial velocity for the continuous flow at the center of the channel is of the so-called parabolic effect, the maximum axial velocity for a fast oscillating flow occurring close to the wall is of the so-called annular effect [17]. Also the transition from laminar to turbulence in reciprocating flow is different for that of continuous flow. Even though the categorization of reciprocating flow regime as either laminar or turbulent is based on the Reynolds number, the definition of the critical Reynolds number for the reciprocating flow in the main pipe is given by:

$$Re_{\omega} = \frac{\omega D^2}{v} \tag{6}$$

While the Reynolds number for the reciprocating flow in the rectangular channels for the cold plate is determined as:

$$(Re_{\omega})_x = \frac{\omega x_{\max}^2}{v} \tag{7}$$

where $x_{\max}$ represents the maximum displacement of the fluid defined by assuming that the fluid moves as a plug flow. In this case, it is equal to the minimum theoretical length of the channel. This value of the Reynolds number in the pipe indicates that the flow in the pipe is

turbulent. As the hydraulic diameter of the cold plate is small than the diameter of the pipe, it follows that the flow in the rectangular channels in the cold plate is turbulent.

The second basic parameters dictating the effect of the oscillating fluid flow frequency [18] is the Wimberley (α) number and the depth of penetration of the flow (δ). At low, the flow is quasi-steady, i.e., the fluid particles everywhere respond instantaneously to the applied pressure gradient. When α is large as in the case of this study case, the motion of the boundary layer follow the pressure gradient more closely than the laminae of fluid in the tube core, which shows phase lags to the imposed pressure gradient. Based on the fluid flow in the cold plate, the two terms are defined as follows:

$$\alpha = \frac{D}{2}\sqrt{\frac{\omega}{\nu}} \tag{8}$$

$$\delta = \sqrt{\frac{2\nu}{\omega}} = \frac{D\sqrt{2}}{\alpha} = depth\,of\ \ penetration \tag{9}$$

For a given reciprocating mechanism-driven heat loop, the volume displacement of the reciprocating driver must be sufficiently large so that the liquid can be supplied from the condenser section to the evaporator section. We wish to find a relation that could describe this critical requirement for the operation of the heat loop. Consider a reciprocating mechanism–driven heat loop under a two-phase working condition (liquid and vapor coexist) similar to that shown in **Figure 5(a)**. The heat loop is assumed to have a condenser section on each side of the reciprocating driver, and the loop is symmetric about the line connecting the midpoints of the evaporator and reservoir. Because of this geometric symmetry, we would like to concentrate on the right half of the loop, as shown in **Figure 5(b)**. The length and average interior cross-sectional area of the evaporator are denoted by L_e and A_e, respectively, the length and average interior cross-sectional area of the connection tubing between the evaporator and the condenser are L_t and A_t, the length and interior cross-sectional area of each condenser section are L_c and A_c, the interior volume of the section between the end of the condenser and the piston right dead center is $V_d/2$, and the piston cross-sectional area and reciprocating stroke are A_p and S, respectively.

2.1. Critical displacement of the reciprocating driver

Consider initially the circuits of both solenoids are open and the piston is stationed in the mid-section of the liquid reservoir, and the vapor generated in the evaporator section pushes the liquid toward the condenser section with a liquid–vapor interface as indicated in the figure. Although there could be thin liquid films at the interior surface of the evaporator, the amount of liquid associated is neglected in the current analysis. In the derivation of the critical liquid displacement, the critical working condition is assumed to be reached when the liquid at the center of condenser, denoted by A, can just reach the mid-section of the evaporator when the right-hand solenoid is turned on and the piston reaches the right dead center in the reservoir.

http://dx.doi.org/10.5772/62518

This condition means that the liquid initially at the condenser center would move to or pass the center of the evaporator as indicated in **Figure 5b**, if the reciprocating mechanism–driven heat loop would work properly. A liquid balance between these two states would give the following relation:

$$A_p.\frac{S}{2}+\frac{V_d}{2}+A_cL_c+A_tL_i \geq \frac{V_d}{2}+A_cL_c+A_tL_t+\frac{1}{2}A_eL_e+\frac{1}{2}A_cL_c+A_tL_i \tag{10}$$

Canceling out the common terms on both sides of the equation and multiplying the resulting equation by 2, we have

$$A_p.S \geq A_cL_c+2A_tL_t+A_eL_e \tag{11}$$

The above equation can be rewritten as follows:

$$A_p.S \geq 2\left(\frac{1}{2}A_cL_c+A_tL_t+\frac{1}{2}A_eL_e\right) \tag{12}$$

The terms in the parentheses on the right-hand side of Equation (12) is the interior volume from the center of the condenser to the center of the evaporator on each side of the heat loop, which reflects one of the essential geometric characteristics of the heat loop in connection with

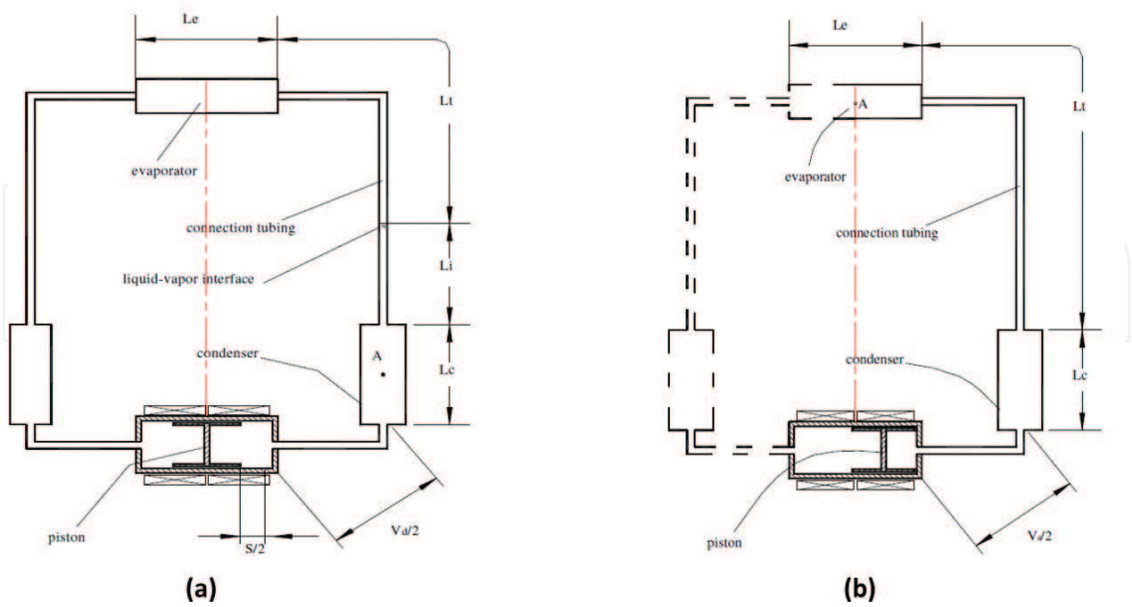

Figure 5. (a) The initial state of the heat loop for the derivation of the working criterion and (b) final state of the heat loop for the derivation of the working criterion [12].

the heat transfer distance and fluid displacement volume. If an effective displacement volume is defined for the entire heat loop as follows:

$$V_{eff} = 2\left(\frac{1}{2}A_cL_c + A_tL_t + \frac{1}{2}A_eL_e\right) \tag{13}$$

Equation (12) can be written as

$$A_p.S \geq V_{eff} \tag{14}$$

Equation (5) indicates that the liquid displacement volume of the piston as represented by A_p.S must be equal to or greater than the effective displacement volume of the heat loop if the heat loop is to work properly. Equation (5), however, is true only for a single-phase heat transfer mode. For a two-phase heat transfer mode, the criterion as represented by Equation (4) or (5) is too conservative because of several reasons. Since the cross-sectional area of the reservoir is usually much greater than that of the rest of the heat loop, the liquid velocity exiting the liquid reservoir should be relatively high. Even if after the piston has reached the dead center in the reservoir, the liquid would continue to move toward the evaporator until the kinetic energy associated with it is exhausted. Additionally, once the liquid enters the evaporator section, some liquid will be evaporated into vapor. The evaporation will drastically change the volume of the flow stream and the liquid/vapor two-phase mixture will expand vigorously into the evaporator section. As a result, the section between the piston right dead center and the center of the evaporator would be filled with both liquid and vapor and the flow is in a two-phase flow condition. It is understood that the liquid fraction would change substantially along the loop. For the derivation of a more concise relation, an effective liquid fraction, $\varnothing$, is used. By taking into account the two-phase flow condition, the liquid balance as represented by Equation (1) should be modified as follows:

$$\begin{aligned} A_p.\frac{S}{2} + \frac{V_d}{2} + \varnothing A_cL_c + \varnothing A_tL_i \geq \frac{V_d}{2} + \\ \varnothing\left(A_cL_c + A_tL_t + \frac{1}{2}A_eL_e + \frac{1}{2}A_cL_c + A_tL_i\right) \end{aligned} \tag{15}$$

Following the same deriving procedure, the following relation is obtained:

$$A_p.S \geq 2\varnothing\left(\frac{1}{2}A_cL_c + A_tL_t + \frac{1}{2}A_eL_e\right) \tag{16}$$

or

http://dx.doi.org/10.5772/62518

$$A_p.S \geq \varnothing V_{eff} \tag{17}$$

The value of ∅, by definition, is greater than zero and less than unity. An actual value of ∅, however, has to be determined experimentally for most practical applications because of the complex heat transfer process in the heat loop. Still, Equation (3) or (7) provides a concise criterion that could be used for the design of a heat loop. It should be pointed out that during the derivation of above relations, the liquid reservoir is assumed to contain pure liquid and the back flow through the gap between the outer surface of the piston and the inner surface of the reservoir casing is neglected. If the reservoir would deal with a two-phase liquid–vapor mixture and the back flow effect is taken into account, the term A_p.S in the above equations may need to be multiplied by a driver efficiency η that is less than unity:

$$\eta A_p.S \geq 2\varnothing\left(\frac{1}{2}A_cL_c + A_tL_t + \frac{1}{2}A_eL_e\right) \tag{18}$$

2.2. Velocity profile

Considering the oscillating motion of the fluid in a pipe that is driven by the sinusoidal varying pressure gradient given by Equation (6), the exact solution of the axial velocity profile for a fully developed laminar reciprocating flow in a circular in a circular pipe is given as [17]:

$$\mathbf{u(r,\ t)} = \frac{\mathbf{A_t}}{\omega}(\mathbf{A\cos(\omega t)} - (1-\mathbf{A})\sin(\omega \mathbf{t})) \tag{19}$$

$$\mathbf{A} = \frac{\mathbf{ber\lambda bei(2\lambda R) + bei\lambda ber(2\lambda R)}}{\mathbf{ber^2\lambda + bei^2\lambda}} \tag{20}$$

$$\mathbf{B} = \frac{\mathbf{ber\lambda bei(2\lambda R) - bei\lambda ber(2\lambda R)}}{\mathbf{ber^2\lambda + bei^2\lambda}} \tag{21}$$

$$\overline{\overline{V}} = \frac{V_{max}}{\tau R}\int_0^R\int_0^\tau\left(\frac{32}{r\sigma Re_\omega}\left[\sin t - \left(e^{-E}\right)\sin\left(t-E\right)\right]\right) \tag{22}$$

And

$$E = \left[1 - \left(\frac{r}{R}\right)^2\right]\sqrt{\frac{Re_\omega}{8}} \tag{23}$$

$$\sigma = \frac{8}{\alpha^3}\sqrt{\left(\alpha - 2C_1\right)^2 + 4C_2^2} \tag{24}$$

$$C_1 = \frac{ber\alpha bei'\alpha - bei\alpha ber'\alpha}{ber^2\alpha + bei^2\alpha} \tag{25}$$

$$C_2 = \frac{ber\alpha bei'\alpha + bei\alpha ber'\alpha}{ber^2\alpha + bei^2\alpha} \tag{26}$$

ber( ), *bei( )*, *ber'( )*, and *bei'( )* are Kelvin functions [19].

2.3. Bulk temperature on the cold plate

An effective tool for comparing the performance of the both of the RMDHL is the value of the bulk temperature on the cold plate. The classical definition of the bulk fluid temperature is given as follows:

$$\boldsymbol{T_b} = \frac{\frac{1}{\boldsymbol{H}}\int_{-\boldsymbol{H}/2}^{\boldsymbol{H}/2} \boldsymbol{V}\left(\boldsymbol{y.t}\right)\boldsymbol{T}\left(\boldsymbol{x},\boldsymbol{y},\boldsymbol{z}\right)\,\boldsymbol{dy}}{\frac{1}{\boldsymbol{H}}\int_{-\boldsymbol{H}/2}^{\boldsymbol{H}/2} \boldsymbol{V}\left(\boldsymbol{y.t}\right)\,\boldsymbol{dy}} \tag{27}$$

$$\overline{\boldsymbol{T_b}} = \frac{\frac{1}{\boldsymbol{\tau H}}\int_{-\boldsymbol{H}/2}^{\boldsymbol{H}/2}\int_0 \boldsymbol{V}\left(\boldsymbol{y.t}\right)\boldsymbol{T}\left(\boldsymbol{x},\boldsymbol{y},\boldsymbol{z}\right)\,\boldsymbol{dy}\,\boldsymbol{dt}}{\overline{\overline{V}}} \tag{28}$$

2.4. Pressure drop friction coefficients

The friction coefficient in Equation (19) needs to be evaluated. For the sake of simplicity, the study is restricted to fully developed steady flow and assumes that the two-phase gas flow is incompressible. There are two components to the wall because of the mixture flow and the interfacial shear stresses, hence the pressure loss friction coefficient.

$$\frac{1}{\sqrt{c_{fW}}} = 3.48 - 4\log_{10}\left[\frac{2k_w}{Dh} + \frac{9.35}{\mathrm{Re}\sqrt{c_{fW}}}\right] \tag{29}$$

http://dx.doi.org/10.5772/62518

We use the single-phase flow relationship to predict the wall friction factor for the gas and liquid phase. If we accept that the momentum transfer across a rough liquid surface is governed by the same mechanism as for a rough wall, it is possible to define the pressure loss friction coefficient as [20]:

$$\frac{1}{\sqrt{c_{fW}}} = 3.48 - 4\log_{10}\left[\frac{2k_W}{D_h} + \frac{9.35}{\mathrm{Re}\sqrt{c_{fW}}}\right] \tag{30}$$

in which k_W is the sand roughness of the wall. If we assume a smooth wall,

$$\frac{1}{\sqrt{c_{fW}}} = 3.48 - 4\log_{10}\left[\frac{9.35}{\mathrm{Re}\sqrt{c_{fW}}}\right] \tag{31}$$

where is the friction coefficient that is related to the friction factor by $f = 4c_f$. The Reynolds number in Equation (20) is based on the mixture density and viscosity:

$$\mathrm{Re} = \frac{VD_h\rho}{\mu} \tag{32}$$

$$\frac{1}{\rho} = \frac{x}{\rho_v} + \frac{1-x}{\rho_l} \tag{33}$$

$$\mu = \frac{x}{\mu_v} + \frac{1-x}{\mu_l} \tag{34}$$

The interfacial pressure drop friction coefficients are determined using the correlation below [20]:

$$\frac{1}{\sqrt{c_{fi}}} = 3.48 - 4\log_{10}\left[\gamma Fr_G f_i + \frac{9.35}{\mathrm{Re}_G\sqrt{c_{fi}}}\right] \tag{35}$$

where Fr_G is a Froude number defined as:

$$Fr_G = \frac{\left(u_g - u_l\right)^2}{gD_{hg}} \tag{36}$$

If we assume that $u_g = u_l$, the equation reduces to

$$\frac{1}{\sqrt{c_{fi}}} = 3.48 - 4\log_{10}\left[\frac{9.35}{\mathrm{Re}_G\sqrt{c_{fi}}}\right] \tag{37}$$

2.5. Heat transfer coefficient

Zhao and Cheng [21] obtained the following correlation for a space cycled averaged Nusselt number for a reciprocating laminar flow as:

$$\overline{Nu} = .02\left(\frac{x_{\max}}{D}\right)^{0.85}\mathrm{Re}_{\omega}^{0.58} \tag{38}$$

where $x_{\max}$ is the maximum fluid displacement within the pipe, and

$$\overline{Nu} = \frac{qD_i}{k_f\left(\overline{T_w} - \overline{T_m}\right)} \tag{39}$$

$\overline{T_w}$ and $\overline{T_m}$ are the bulk temperatures for the cold plate and coolant, respectively.

3. Performance comparison of RMDHL to CONTINUOUS cooling system

In this section heat transfer and fluid flow aspects of the reciprocating mechanism–driven heat loops (RMDHL) have been studied numerically using the available commercial software, Ansys Fluent [22]. The main objective of the present study is to compare the performance of a RMDHL with the conventional continuous cooling loops in terms of temperature, uniformity, and heat removal from the surface of the heat source. For the current study, 3D setup of CONTINUOUS and RMDHL cooling loops are provided. The 3D setup, which is based on the previous experimental studies, can be used for future development and optimization of a real industrial product.

http://dx.doi.org/10.5772/62518

3.1. Numerical study of continuous cooling loops

Figure 6 shows the geometrical and boundary conditions of the cooling loops. Both loops are consisting of a single passage with two 90′ elbows. The inner loop is the condenser loop and the other loop forms the evaporator loop. The condenser and evaporator loops are enclosed with solid wall.

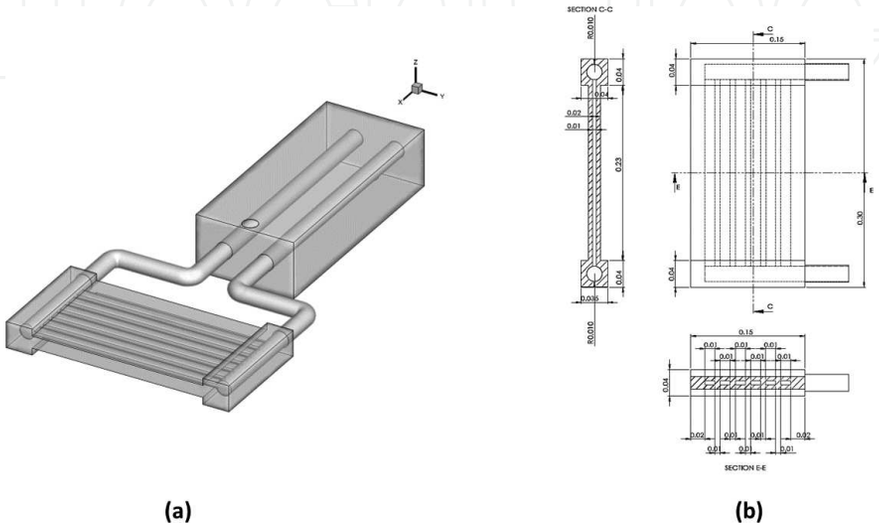

Figure 6. (a) 3D geometry of the cooling loops and (b) key dimensions.

The two loops are the main challenge in the present simulation to setup a closed loop in Ansys fluent. Based on the Navier Stokes equation, the continuity and momentum equations are coupled and for an incompressible flow, and the SIMPLE algorithm indicates the coupling of pressure and momentum fields inside the computational domain. Hence introducing a cross section with a constant velocity in a closed loop would result in a discontinuity in the velocity field, which makes the solution unstable and leads to inaccurate results. **Figure 7** shows the grid distribution for the present simulation.

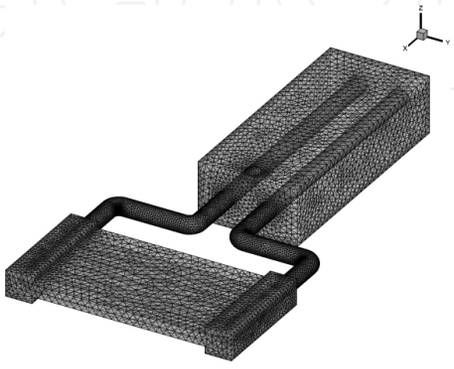

Figure 7. Mesh distribution for a 3D.

Hence, the CONTINUOUS loops are simulated using the following setups:

For continues loop:

a. Instead of a closed loop, an open loop is simulated.

b. Constant velocity is applied on the inlet boundary to obtain the same flow rate.

c. Using a User Defined Function (UDF), the inlet temperature of the loop is set as the average outlet.

Temperature of the loop should mimic the temperature and velocity of a closed loop. The solid walls are copper, and their thermophysical properties are obtained from the fluent database. The working liquid in the both loops is water.

3.2. Governing equations and boundary condition

In the present study for the CONTINUOUS loop the following assumptions are made:

1. Both fluid flow and heat transfer are in steady-state.

2. Fluid is in single phase and flow and laminar.

3. Properties of both fluid and heat sink materials are temperature independent.

4. All the surfaces of heat sink exposed to the surroundings are assumed to be insulated except the walls of evaporator where constant heat flux simulating the heat generation from different components.

Based on above assumptions, the governing equations for fluid and energy transport are:

Fluid flow:

$$\nabla \cdot \vec{V} = 0 \tag{40}$$

$$\rho\left(\vec{V} \cdot \nabla V\right) = -\nabla p + \mu \nabla^2 \vec{V} \tag{41}$$

Energy in fluid flow:

$$\rho c_p \left(\vec{V} \cdot \nabla T\right) = k \nabla^2 T \tag{42}$$

Based on the operating conditions described above, the boundary conditions for the governing equations are given as:

Inlet:

http://dx.doi.org/10.5772/62518

$$V = V_{in}, \quad T_{in} = \left(T_{out}\right)_{ave} \tag{43}$$

Outlet:

$$P = P_{out}, \quad \frac{\partial T}{\partial n} = 0 \tag{44}$$

Fluid–solid interface:

$$\vec{V} = 0, \quad T = T_s, \quad -k_s \frac{\partial T_s}{\partial n} = -k \frac{\partial T}{\partial n} \tag{45}$$

At the top wall:

$$q_w = -k_s \frac{\partial T_s}{\partial n} \tag{46}$$

In Equation (44), V_{in} and T_{in} are the fluid inlet pressure and temperature, respectively; p_{out} is the pressure at the outlet, n is the direction normal to the wall or the outlet plane, and q_w is the heat flux applied at the top wall of the heat sink.

3.3. Numerical studies of RMDHL cooling loops

The geometry and grid distribution for RMDHL is as same as CONTINOUS loop. To simulate a closed RMDHL loop, the following setup is used:

For RMDHL loop:

a. Instead of a closed loop, an open loop is simulated.

b. A UDF is used to generate the sinusoidal inlet velocity for the evaporator loop.

c. Using a UDF, the inlet temperature of the loop is set as the average outlet temperature of the loop and the backflow temperature of the outlet is set to the average temperature of the inlet boundary to mimic the temperature and velocity in distribution of a closed loop.

4. Performance of CONTINOUS and RMDHL loops

Temperature profiles on the evaporator walls (left and right walls) are also shown in **Figure 8b**, **d**, **f**, and **h**. The figures clearly show the non-uniformity of the temperature contours for the CONTINOUS loop. As seen in these figures, the temperature is minimum at the inlet

of the evaporator and gradually increases toward the outlet of the outlet. Moreover, these figure clearly indicate that the temperature increases with increase in heat flux on the walls.

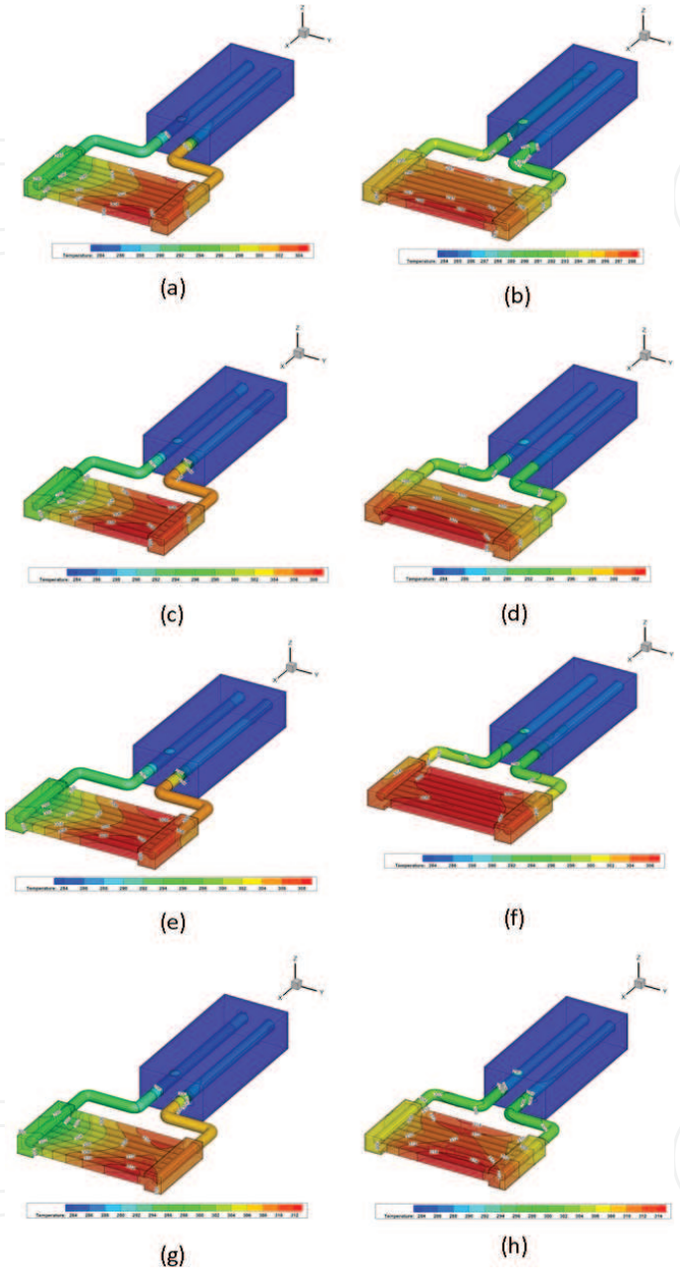

Figure 8. Temperature profile on the evaporator surface, T = 30 s for heat fluxes (a), (b) 11594.2 W/m^2 (c), (d) 13043.48 W/m^2, (e),(f) 14492.75 W/m^2, and (g),(h) 15971.01 W/m^2.

Contrary to the CONTINOUS loop, the temperature contour is in symmetry for a RMDHL system. The temperature distributions of both the RMDHL and CONTINOUS cold plates are obtained at a condenser inlet velocity of 1.23 m/s, heat transfer rate range from 11594 W/m^2, and 15971 W/m^2 and a condenser inlet temperature of 283 K. The results of unsteady simulation in **Figures 8a, c, e**, and **g** indicate the following important point:

1. Frequency of the inlet velocity has a very important effect on the rate of heat removal from the evaporator. In fact, it can be concluded the optimum loop time should be equal or more than:

$$\Delta T = 2 \times \Delta T_{half} \tag{47}$$

Where

$$\Delta T_{half} = \frac{L_{half}}{U_{max}} \tag{48}$$

Where L_{half} is the half of the evaporator loop length and $U_{\max}$ is the maximum velocity of the fluid in evaporator loop. The numerical results also show that choosing the duration time less than the above value results in much higher temperature on the evaporator walls because the fluid could not transfer the heat from the evaporator to the condenser well.

2. In this study a sinusoidal velocity profile is used, but there is no guarantee that this profile is the best choice to obtain the maximum heat transfer rate. The authors believe that a velocity profile with longer residence time and shorter circulation time will have a better performance for the RMDH loops.3. In this study a reciprocating velocity profile has been applied on the inlet boundary and out let boundary is set to constant pressure boundary.

Figures 8 a–h clearly show that the uniformity of the temperature profiles of the RMDHL shown in the left column is much better than that of the CONTINOUS. As seen in **Figures 8**, there are two temperature gradients: one gradient along the evaporator width and the another gradient across the evaporator thickness. The gradient along the evaporator width is similar for both the CONTINOUS and the RMDHL and is because of the pressure drop along the grooves in the evaporator. The effect of this gradient can be reduced if a different groove configuration is adopted. However, it is observed that the pressure gradient along the evaporator is more pronounced for the CONTINOUS loop than the RMDHL loop. For the temperature gradient along the fluid flow path, **Figure 8** shows that the CONTINOUS (the column of the right) has up to 13 distinct temperature bands where observed for the 15,971.01 W/m^2 cold plate. It was also observable that temperature band increases with increasing heat flux, whereas for the RMDHL the number of bands is much fewer and independent of heat flux. As much as 80% of the cold plate of the RMDHL was maintained at a within a temperature difference of 0.5 °C.

5. Conclusion

In this chapter the concept of bellows-type and solenoid-based RMDHL cooling mechanism has been demonstrated. This novel type of cooling system has several advantages over the

conventional cooling system in power electronic cooling industries. The experimental results clearly showed that the heat loop worked very effectively and a heat flux in the evaporator section could be handled. Moreover, it has been proven both numerically and theoretically that the RMDHL provides superior cooling advantage with respect to temperature uniformity compared with CONTINOUS cooling loops; hence it could be an alternative of a conventional liquid cooling system (LCS) for electronic cooling applications. The results also proved that the bellows-type RMDHL has successfully overcome the weakness of small displacement of a solenoid-based RMDHL, and enabled a RMDHL for applications involving large heat transfer rates and over a large surface area. The tests also show that the bellows-type RMDHL has the potential to maintain a heat-generating surface at an exceedingly uniform temperature. Although in some cases, the maximum temperature difference over the cold plate has exceeded, this temperature difference may be significantly reduced with a more powerful actuator working at a higher frequency. The power consumption of the bellows driver was less than 5 W in all cases, resulting in a ratio of the driver power input to the heat input of the cold plate being less than 1%, which is a ten-fold improvement over that of the solenoid-based RMDHL. Using numerical analysis, CONTINOUS and RMDHL loops are simulated as well. The numerical simulations have been conducted using different parameters and boundary conditions for a 3D setup. The results show that the temperature increases with an increase in heat flux on the walls or decrease of the flow rate. The results also indicate that the temperature profiles are more uniform for an RMDHL loop compared with a CONTINOUS loop.

Nomenclature

A	Area [m^2]
C_p	Specific heat [J/kg K]
D_i	Inside tube diameter [m]
D_o	Tube outside diameter [m]
D_h	Hydraulic diameter [m]
H	Height of rectangular channel [m]
h	Heat-transfer coefficient [W/m^2 K]
k	Thermal conductivity [W/m^{2}K]
L	Length
n	Reciprocating pump stroke frequency[cycles/s]
$\dot{m}$	Mass flow rate [kg/s]
Nu	Nusselt number: $h/(k/D_h)$
p	Pressure [Pa]
$\dot{Q}$	Heat transfer rate [W]
σ_T	Standard deviation
α	Surface effectiveness: $\sqrt{2\nu/\omega}$
μ	Dynamic viscosity [kg/ms]
ρ	Density [kg/m^3]
ω	pump frequency [rad/s]
τ	Cycle period [s]
σ	Constant: $(8/\alpha^3)\sqrt{(\alpha-2C_1)^2+4C_2^2}$

Subscript

ave	Average value
c	Condenser
e	Evaporator
in	Inlet
m	Mean value
min	Minimum value

http://dx.doi.org/10.5772/62518

Nomenclature

q	Volume flow rate [m^3/s]
Re	Reynolds number: $(\rho VD)/\mu$
Re_ω	Kinetic Reynolds number: $\omega x_{max}^2 / v$ [m]
r	Tube inside radius [m]
S	Stroke [m]
T	Temperature [°C]
U	Overall heat-transfer coefficient[W/m^2 K]
t	Time[s]

Greek Letters

s	Flow penetration

max	Maximum value
n	Direction normal to the wall
out	Outlet
p	Pump piston
s	Surface
t	Tubing
w	Wall

Superscript

= -	Time-averaged quantity
→	Vector

Author details

Olubunmi Popoola, Soheil Soleimanikutanaei* and Yiding Cao

*Address all correspondence to: ssole016@fiu.edu

Department of Mechanical Materials Engineering, Florida International University, Miami, Florida, USA

References

[1] Semiconductor Industry Association. International Technology Roadmap for Semiconductors. Austin, TX: International SEMATECH; 1999.

[2] Zuo Z, Hoover L, and Phillips A. Thermal Challenges in Next Generation Electronic Systems, 317–336. Joshi, Y.K., Garimella, S.V. An integrated thermal architecture for thermal management of high power electronics, Millpress, 2002, 416. http://www.iospress.nl/book/thermal-challenges-in-next-generation-electronic-systems/ 978-90-77017-03-6

[3] Vafai K. High heat flux electronic cooling apparatus, devices and systems incorporating same. US 20020135980A1. 2002.

[4] Bergles AEA. High-flux processes through enhanced heat transfer. 2003; http://dspace.mit.edu/handle/1721.1/5564.

[5] Liu Z, Tan S, Wang H, Hua Y, and Gupta A. Compact thermal modelling for packaged microprocessor design with practical power maps. Integration the VLSI Journal. 2014;47(1):71–85.

[6] Hetsroni G, Mosyak A, and Segal Z. Nonuniform temperature distribution in electronic devices cooled by flow in parallel microchannels. IEEE Transactions on Components and Packaging Technologies. 2001;24(1):16–23.

[7] Krishnamoorthy S. Modeling and Analysis of Temperature Distribution in Nanoscale Circuits and Packages. Chicago: University of Illinois; 2008.

[8] Jeakins W and Moizer W. Cooling of electronic equipment. US Pat; 2003. 1–70.

[9] Cao Y, Xu D, and Gao M. Experimental study of a bellows-type reciprocating-mechanism driven heat loop. International Journal of Energy Research. 2013;37(6):665–672.

[10] Faghri A. Heat pipe science and technology. Washington, DC: Taylor & Francis; 1995.

[11] Kosoy B. Heat Pipes. Kirk-Othmer Encyclopedia of Chemical Technology. 19 Nov 2004. 1–20. http://onlinelibrary.wiley.com/doi/10.1002/0471238961.0805012002090514.a01.pub2/abstract DOI: 10.1002/0471238961.0805012002090514.a01.pub2.

[12] Cao Y and Gao M. Experimental and analytical studies of reciprocating-mechanism driven heat loops (RMDHLs). Journal of Heat Transfer. 2008;130(7):1–20.

[13] Munson B, Young D, and Okiishi T. Fundamentals of Fluid Mechanics. 6th edition. Danvers: Wiley; 2009.

[14] Cao Y and Wang Q. Engine Piston. U.S. Patent No. 5,454,351. 3 October 1995.

[15] Cao Y and Gao M. Reciprocating-mechanism driven heat loops and their applications. ASME 2003 Heat Transfer Summer Conference. 2003.

[16] De-Jongh J and Rijs R. Pump Design. Arrakis; 2004.

[17] Zhao TS and Cheng P. Heat transfer in oscillatory flows. Annual Review of Heat Transfer. 1998;4(35):359–419.

[18] Menon AS, Weber ME, and Chang HK. Model study of flow dynamics in human central airways. Part III: Oscillatory velocity profiles. Respiration Physiology. 1984;55(2):255–275.

[19] Uchida S. The pulsating viscous flow superposed on the steady laminar motion of incompressible fluid in a circular pipe. J Zeitschrift für Angew. Math. und Phys ZAMP. 1964;19(1):117–120.

[20] Line A and Fabre J. Stratified gas–liquid flow. in International Encyclopaedia of Heat and Mass Transfer, Hewitt GF, Shires GL, CRC Press, 1997.1097-1101

[21] Zhao TS and Cheng P. Oscillatory heat transfer in a pipe subjected a periodically reversing flow. ASME Journal of Heat Transfer. 1996;118:592–598.

[22] Available from: http://www.ansys.com/.